5-1-2016

Is Cell Viability Always Directly Related to Corrosion Resistance of Stainless Steels?

E. Salahinejad
K.N.Toosi University of Technology

M. Ghaffari
Bruker AXS, Inc.

Daryoosh Vashaee
North Carolina State University

Lobat Tayebi
Marquette University, lobat.tayebi@marquette.edu

Accepted version. *Materials Science and Engineering: C,* Vol. 62 (May 1, 2016): 439-443. DOI.

Is Cell Viability Always Directly Related to Corrosion Resistance of Stainless Steels?

E. Salahinejad
Faculty of Materials Science and Engineering, K.N. Toosi University of Technology, Tehran, Iran
M. Ghaffari
Bruker AXS Inc., Madison, WI
D. Vashaee
Electrical and Computer Engineering Department, North Carolina State University, Raleigh, NC
L. Tayebi
School of Dentistry, Department of Developmental Sciences, Marquette University, Milwaukee, WI
Department of Engineering Science, University of Oxford, Oxford, UK

Materials Science and Engineering: C, Vol 62 (May 1, 2016): pg. 439-443. DOI.

Abstract: It has been frequently reported that cell viability on stainless steels is improved by increasing their corrosion resistance. The question that arises is whether human cell viability is always directly related to corrosion resistance in these biostable alloys. In this work, the microstructure and in vitro corrosion behavior of a new class of medical-grade stainless steels were correlated with adult human mesenchymal stem cell viability. The samples were produced by a powder metallurgy route, consisting of mechanical alloying and liquid-phase sintering with a sintering aid of a eutectic Mn–Si alloy at 1050 °C for 30 and 60 min, leading to nanostructures. In accordance with transmission electron microscopic studies, the additive particles for the sintering time of 30 min were not completely melted. Electrochemical impedance spectroscopic experiments suggested the higher corrosion resistance for the sample sintered for 60 min; however, a better cell viability on the surface of the less corrosion-resistant sample was unexpectedly found. This behavior is explained by considering the higher ion release rate of the Mn–Si additive material, as preferred sites to corrosion attack based on scanning electron microscopic observations, which is advantageous to the cells in vitro. In conclusion, cell viability is not always directly related to corrosion resistance in stainless steels. Typically, the introduction of biodegradable and biocompatible phases to biostable alloys, which are conventionally anticipated to be corrosion-resistant, can be advantageous to human cell responses similar to biodegradable metals.

Keywords: Nanostructures, Medical-grade stainless steels, Corrosion, Stem cell viability

1. Introduction

One of the main requirements for any biomaterial is biocompatibility, the term which refers to a collection of interactions between the material and body tissues. Analyzing cell attachment and viability on surfaces is currently regarded as an essential indicator of biocompatibility.[1,2,3] This cell/substrate interaction is affected by different features of the biomaterial's surface, including roughness, wettability, released species type, and ion release rate.[4,5,6,7,8,9] Among them, it is known that the ion release rate can be directly related to corrosion rate, especially uniform corrosion instead of localized types.[10,11] Thus, electrochemical corrosion measurements like impedance spectroscopy (EIS) and potentiodynamic polarization, measuring uniform corrosion rate, can be used to qualitatively estimate and compare cell viability.[10,11,12]

With regard to biodegradable metallic biomaterials like magnesium-based alloys, corrosion products fundamentally are advantageous to biological processes, since released ions are essential

species for the body and help healing mechanisms.[13,14,15] However, for the conventionally used metallic biomaterials designed to be biostable, including stainless steels (AISI 316L), corrosion is deleterious to the body. This is due to the fact that these alloys are composed of some elements that are harmful to the body, especially at high ion release rates.[16] For example, nickel is known to cause allergic reactions on the skin. To resolve this issue, nickel-free stainless steels are being developed.[16,17,18,19,20] Note that the corrosion produces of other constitutes can be still disadvantageous when releasing at high levels, for example chromium.

In ASTM standards, two nickel-free medical-grade stainless steels have been introduced: ASTM ID: F2229 and ASTM ID: F2581. Recently, the structure and some properties of powder metallurgy (mechanical alloying and liquid-phase sintering) samples with the latter standard composition were investigated.[21,22,23] Typically, it was found that a higher resistance to uniform corrosion, estimated from EIS experiments, dictates a more cell viability on the surfaces, albeit when liquid-phase sintering was completely activated.[10] Nevertheless, the question is whether this conclusion is universal, i.e. whether corrosion resistance is always directly related to human cell viability for this type of alloys. This study focuses on this null hypothesis, where this correlation for complete and incomplete liquid-phase sintering of a medical-grade nickel-free stainless steel was checked.

2. Experimental procedure

Nickel-free stainless steel powders with the chemical composition of ASTM ID: F2581 (Fe–17Cr–10Mn–3Mo–0.4Si–0.5N–0.2C) were first prepared by mechanical alloying, then mixed with 3 wt.% of pre-alloyed Mn–11.5Si powders as a liquid-phase sintering agent, and finally sintered at 1050 °C for 30 and 60 min. The elemental chemicals were supplied by Merck, Munchen, Germany. This sintering temperature was selected since the melting point of the eutectic additive is 1040 °C.[21] A scanning electron microscope (SEM, Hitachi S-4800) and transmission electron microscope (TEM, FEI-Tecnai G2F30) equipped with energy dispersive X-ray spectroscopy (EDX) were used to characterize the resultant microstructure after sintering.

Materials Science and Engineering: C, Vol 62 (May 1, 2016): pg. 439-443. DOI.

Electrochemical impedance spectroscopic (EIS) experiments were performed on the samples in the simulated body fluid (SBF)[24] at 37 °C under the naturally aerated condition, after 48 h of immersion in the SBF to get a steady-state condition, over ten frequency decades from 5 kHz to 10 mHz with an excitation potential amplitude of 10 mV at the open circuit potential. Also, the sample surfaces after 15 days of immersion in the SBF were studies by SEM. Three replicates were performed for the corrosion tests.

For the assessment of cell viability, the polished stainless steel samples were sterilized by autoclaving at 134 °C for 20 min. Afterwards, a concentrated (500,000 cells/mL) adult human mesenchymal stem cell (hMSC) suspension was seeded onto the tissue culture plastic (TCP) surface (as the standard) and each sample. After one day, the sample surfaces were fixed in 3.7% formaldehyde for 30 min at room temperature, dried by ethanol, and observed by SEM. On the other hand, the samples were washed in MSCGM and cytoplasmic CFDA-SE stained was extracted from live cells by freezing and thawing. The CFDA-SE content was then assessed by fluorescence intensity in a spectrofluorometer. Quadruplicate samples were used for each condition. Other details on the cell culture and viability testing are available in Ref.[10]

3. Results and discussion

Fig. 1 shows the SEM micrograph of the samples sintered at 1050 °C for 30 and 60 min, where a better densification can be seen for the longer sintering time. The TEM micrographs and EDS spectrum taken of the sample sintered at 1050 °C for 30 min are presented in Fig. 2. According to Fig. 2a, a number of dark islands with different sizes are observed in the bright matrix. Also, the high-magnification TEM micrograph of one of these nanosized islands (Fig. 2b) indicates that there is a compact interface between the matrix and island without any gap. Fig. 2c shows the EDS spectrum of one of the dark regions, suggesting that they are Mn–Si-rich (additive) zones.

Materials Science and Engineering: C, Vol 62 (May 1, 2016): pg. 439-443. DOI.

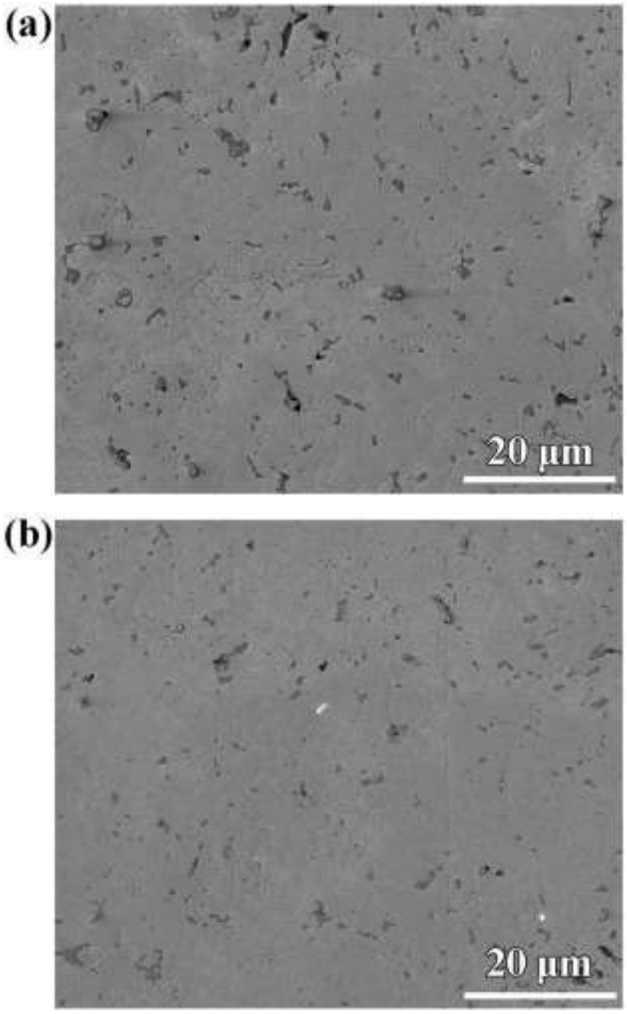

Fig. 1. SEM micrograph of the samples sintered at 1050 °C for 30 (a) and 60 (b) min.

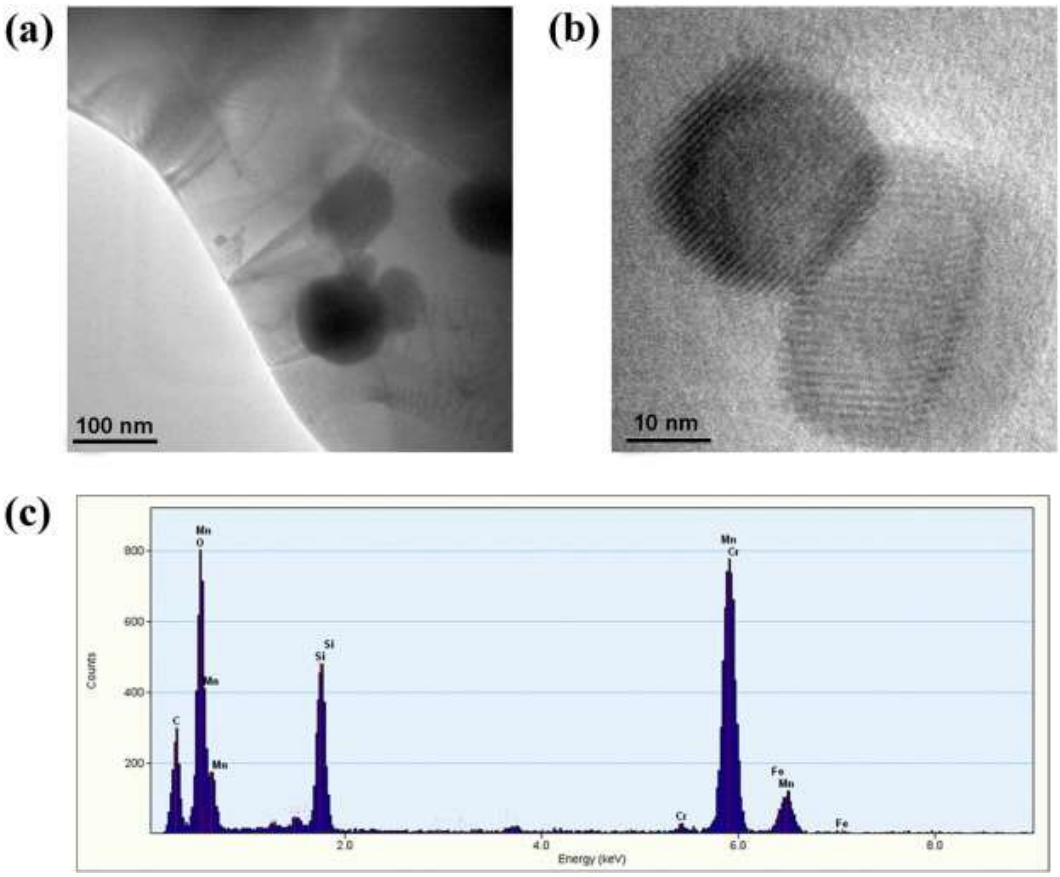

Fig. 2. TEM micrograph (a) of the sample sintered for 30 min, high-magnification TEM micrograph (b) and EDS spectrum (c) of a nanometric dark island in (a).

It can be inferred from these TEM analyses that liquation of the additive has occurred, realized from the interface feature; however, there has not been an enough duration for its complete penetration as they can be still observed as the islands, albeit in ultrafine and nanometric sizes. In other words, as clear in the Mn–Si phase diagram, the additive has to be melted at temperatures beyond 1040 °C. This sample, as noted in the experimental section, experienced the sintering temperature of 1050 °C; thus, the additive liquation and then wetting of stainless steel particles were logically anticipated. However, the complete penetration of the additive into main particle contacts and pore zones via capillary forces kinetically demands a duration at this temperature, which was not satisfied by a sintering time of 30 min, as confirmed by the presence of the island in the micrographs. In contrast, sintering at 1050 °C for 60 min is enough for the complete penetration and obtaining a single-phase structure, as confirmed by TEM and SEM studies elsewhere.[21,25]

Materials Science and Engineering: C, Vol 62 (May 1, 2016): pg. 439-443. DOI.

Cell attachment can be well explained by EIS rather than polarization, where these two electrochemical techniques were compared in.[10] The Bode and Nyquist impedance plots of the samples after immersion in the SBF for 48 h are indicated in Fig. 3. It can be seen that the two samples represent a similar impedance behavior referring to passive systems, according to the Bode and Nyquist plots. According to these curves, the impedance values over the whole frequency range and thereby corrosion resistance for the sintering time of 60 min is higher than those of the 30 min sample. That is, the whole ion release rate of the 30 min sample, including the additive and matrix materials, is higher than that of the 60 min sample. Fig. 4 depicts the SEM micrographs of the sintered sample after 15 days of immersion in the SBF. In the lower magnification image of the 30 min sample (Fig. 4a), some holes can be observed on the surface. A precise consideration to one of the holes (Fig. 4b) suggests that the holes have been created in the gaps of the main powder particles, as can be inferred from grain/particle boundaries at the bottom of the hole and those perpendicular to the circumference of the hole on the surface (shown by arrows). These places had been occupied by the additive particles before corrosion attack. That is, it can be inferred that the Mn–Si additive zones have experienced corrosion damage more considerably and have left holes due to corrosion attack. On the other hand, according to Fig. 4c, the 60 min sample does not show this type of corrosion attack features on its surface, because the additive materials have been completely penetrated into the structure during sintering with the enough duration.

Materials Science and Engineering: C, Vol 62 (May 1, 2016): pg. 439-443. DOI.

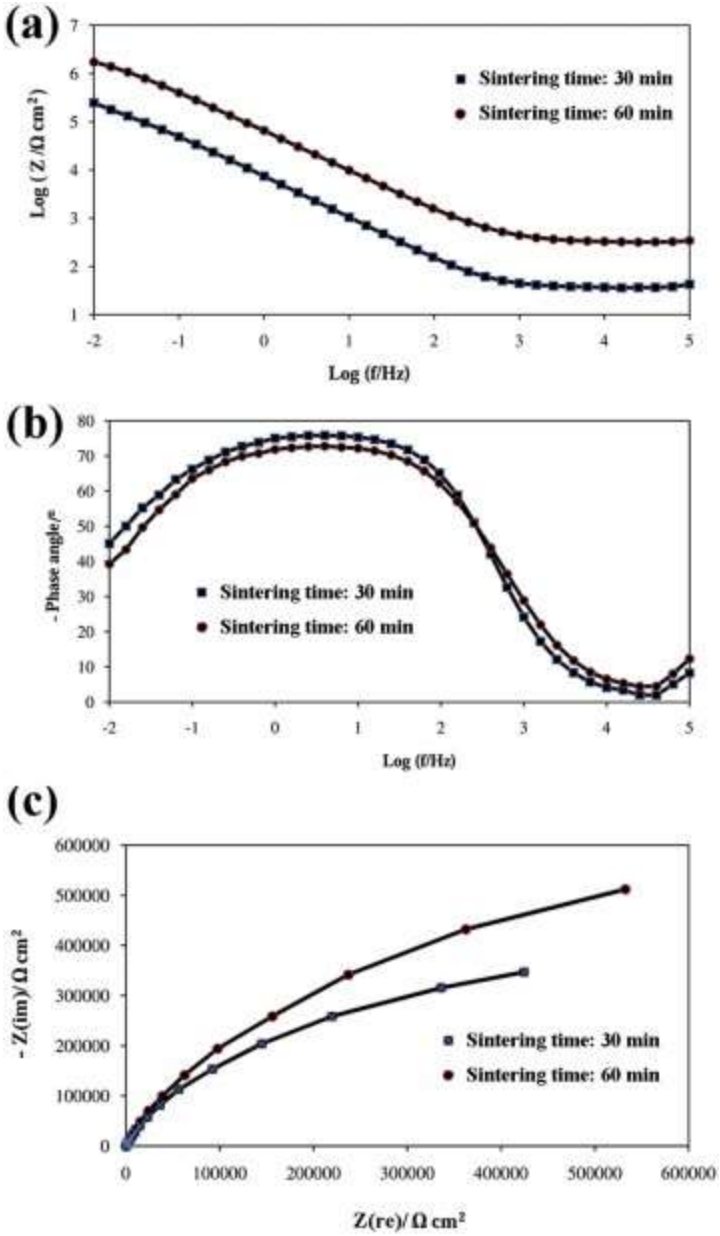

Fig. 3. EIS results of the sample sintered for the different durations: Bode impedance (a), Bode phase angle (b), and (c) Nyquist plots.

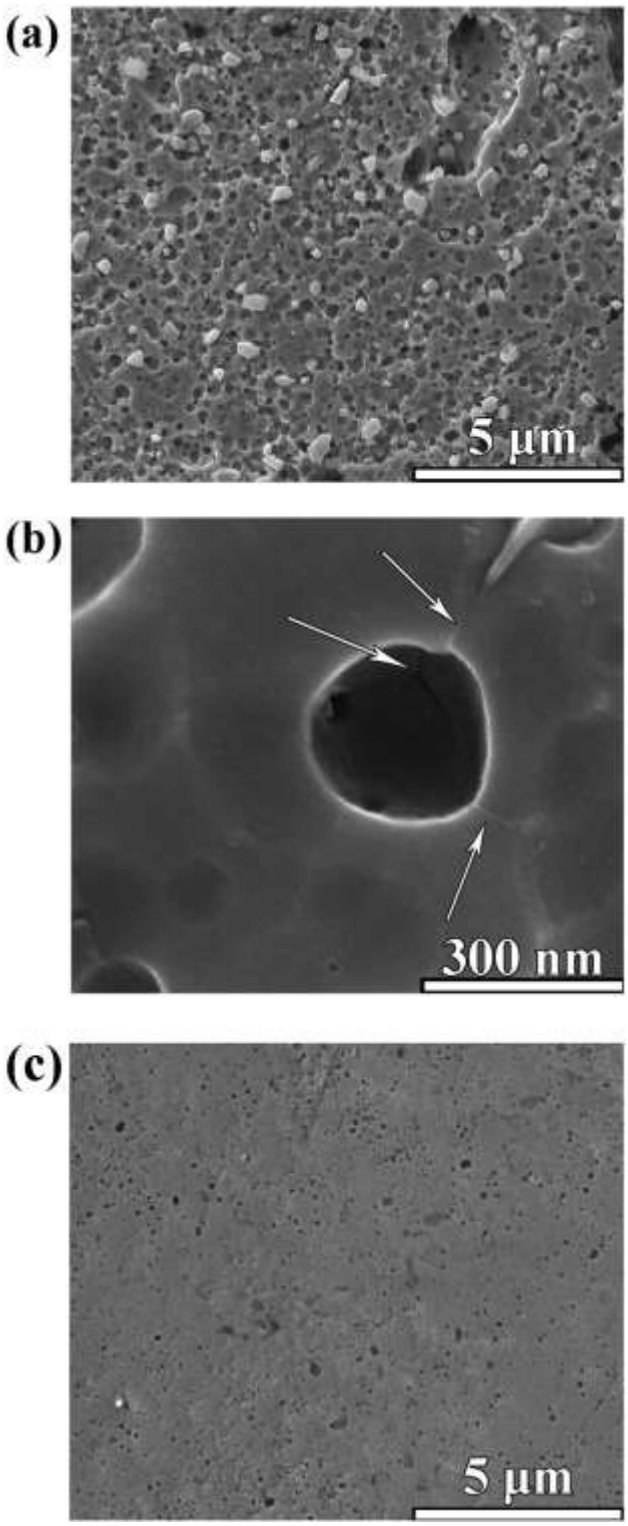

Fig. 4. SEM micrographs of the 30 min sample (a and b) and the 60 min sample (c), after 15 days of immersion in the SBF.

The observed electrochemical behavior can be logically justified by the microscopic studies conducted. As noted above (Fig. 2), in the sample sintered for 30 min, there are some Mn–Si-rich zones. As manganese is not a typical active–passive metal, in contrast to the stainless steel matrix containing chromium,[26] the islands essentially present low corrosion resistance. Indeed, islands act as micro/nanoanodes and are more rapidly corroded, while the stainless steel matrix – which is electrically connected to the anodic areas – acts as a microcathode (cathodic protection), because of their different electrochemical potential. It should be also considered that the islands embrace a small area of the surface compared to the matrix, suggesting the area effect or the ratio of the cathodic to anodic area. The greater the ratio of the cathodic to anodic area, the greater the current density at the anodic area and thereby the greater the corrosion rate.[26] In summary, in the case of the 30 min sample, the ion release rate from the stainless steel matrix containing some harmful elements for the body is lower compared with the 60 min sample, due to cathodic protection by the Mn–Si-rich zones. In return, this sample presents a higher release rate of manganese ions, which is not essentially harmful for the body as the islands were not covered by a passive film mainly created by chromium.

Using pre-staining of the cells with CFDA-SE, the viability of hMSCs on the samples was assessed after one day. The cell viability percents are 99 and 97% relative to TCP for the 30 min and 60 min samples, respectively (experimental error < 1%), which is fairly considerable and comparable to TCP, i.e. they are not toxic to the cells during the chosen culture period. Nevertheless, the cell viability on the 30 min sample is a little more than the other stainless steel sample. These results are also verified by the SEM micrographs taken from cells fixed on the samples, where the cells present a desirable distribution on both of the surfaces in the low-magnification ones (Fig. 5a and b). The SEM micrographs of one cell on the surfaces are also presented in Fig. 5c and d, showing a well-spread feature on both of the surfaces with numerous lamellipodia and filopodia. A comparative consideration to the micrographs, however, suggests that the cell feature on the sample sintered for 30 min is a little more desirable, as confirmed by the quantitative results.

Materials Science and Engineering: C, Vol 62 (May 1, 2016): pg. 439-443. DOI.

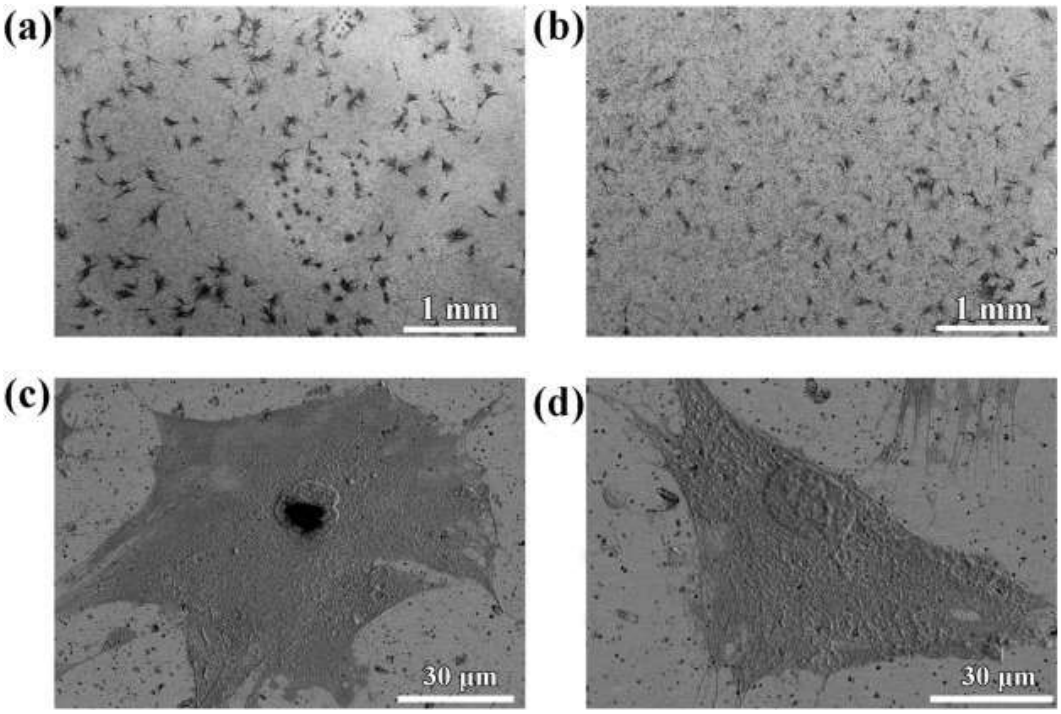

Fig. 5. SEM micrograph of cells fixed on the 30 min (a and c) and 60 min (b and d) samples in different magnifications.

According to the study of the cell viability, the cell attachment on both of the sample was desirable, suggesting the good biocompatibility of the samples due to their composition and good corrosion resistance. The minor difference observed can be speculated by the conclusion drawn from the EIS analysis. The main element in the composition which can be detrimental to the cells is chromium.[17] As noted above, the ion release rate of the stainless steel matrix for the 30 min sample is lower, due to cathodic protection by the unpenetrated additive. In contrast, when the additive is completely dissolved in the stainless steel matrix (for example after 60 min of sintering), the cathodic protection does not occur as the material becomes single-phase and no sacrificial phase is available. Apart from this contribution, as noted in the experimental section, the stainless steel powders were synthesized by mechanical alloying, a process that induces nanocrystallization and amorphization.[27,28,29,30,31,32] During sintering, the shorter duration of the 30 min sample results in lower grain/crystal growth; and the smaller the grain/crystallite size the higher the corrosion rate and ion release rate.[33] albeit from the stainless steel matrix. On the other hand, the release of manganese ions from this sample can be even beneficial to the cells. Thus, it can

be concluded that the presence of an amount of the unpenetrated Mn–Si additive in the structure of the stainless steel, while decreasing the corrosion resistance, can improve the cell viability and thereby biocompatibility.

4. Conclusions

The structure, in vitro electrochemical corrosion, and stem cell viability of two stainless steel samples both liquid-phase sintered at 1050 °C but in different durations (30 min and 60 min) were studied. According to the TEM studies, there were some unmelted Mn–Si sintering aid islands, from a few nano- to micro-meter in size, in the 30 min sintered samples in contrast to the 60 min one. The EIS studies showed that the 60 min sintered sample is more resistant to corrosion due to its uniform structure. The study of the hMSC attachment and viability on the surfaces indicated that both of the samples were relatively similar and desirable substrates for the cells; however, the 30 min sintered sample showed a better behavior to some extent. Eventually, it is concluded that cell viability is not always directly related to corrosion resistance in stainless steels. Indeed, the introduction of biodegradable and biocompatible phases to biostable alloys can be advantageous to human cell responses, as a result of the cathodic corrosion protection of the matrix.

References

[1]M. Chen, P.O. Zamora, P. Som, L.A. Peña, S. Osaki. Cell attachment and biocompatibility of polytetrafluoroethylene (PTFE) treated with glow-discharge plasma of mixed ammonia and oxygen. *J. Biomater. Sci. Polym. Ed.,* 14 (2003), pp. 917–935

[2]M. Assad, N. Lemieux, C. Rivard, L. Yahia. Comparative in vitro biocompatibility of nickel–titanium, pure nickel, pure titanium, and stainless steel: genotoxicity and atomic absorption evaluation. *Bio-Med. Mater. Eng.,* 9 (1998), pp. 1–12

[3]M. Gardel, U. Schwarz. Cell–substrate interactions. *J. Phys. Condens. Matter,* 22 (2010), p. 190301

[4]N.J. Sniadecki, R.A. Desai, S.A. Ruiz, C.S. Chen. Nanotechnology for cell–substrate interactions. *Ann. Biomed. Eng.,* 34 (2006), pp. 59–74

[5]A. Allion, J.-P. Baron, L. Boulange-Petermann. Impact of surface energy and roughness on cell distribution and viability. *Biofouling,* 22 (2006), pp. 269–278

[6]A. Ranella, M. Barberoglou, S. Bakogianni, C. Fotakis, E. Stratakis. Tuning cell adhesion by controlling the roughness and wettability of 3D micro/nano silicon structures. *Acta Biomater.,* 6 (2010), pp. 2711–2720

[7]K. Cai, J. Bossert, K.D. Jandt. Does the nanometre scale topography of titanium influence protein adsorption and cell proliferation? *Colloids Surf. B: Biointerfaces,* 49 (2006), pp. 136–144

[8]J. Bumgardner, L. Lucas. Cellular response to metallic ions released from nickel–chromium dental alloys. *J. Dent. Res.,* 74 (1995), pp. 1521–1527

[9]H. Hermawan, A. Purnama, D. Dube, J. Couet, D. Mantovani. Fe–Mn alloys for metallic biodegradable stents: degradation and cell viability studies. *Acta Biomater.,* 6 (2010), pp. 1852–1860

[10]E. Salahinejad, M.J. Hadianfard, D.D. Macdonald, S. Sharifi-Asl, M. Mozafari, K.J. Walker, A.T. Rad, S.V. Madihally, L. Tayebi. In vitro electrochemical corrosion and cell viability studies on nickel-free stainless steel orthopedic implants. *PLoS One,* 8 (2013), pp. 1–8

[11]E. Salahinejad, M. Hadianfard, D. Macdonald, M. Mozafari, K. Walker, A.T. Rad, S. Madihally, D. Vashaee, L. Tayebi. Surface modification of stainless steel orthopedic implants by sol–gel ZrTiO4 and $ZrTiO_4$–PMMA coatings. *J. Biomed. Nanotechnol.,* 9 (2013), pp. 1327–1335

[12]X. Gu, Y. Zheng, Y. Cheng, S. Zhong, T. Xi. In vitro corrosion and biocompatibility of binary magnesium alloys. *Biomaterials,* 30 (2009), pp. 484–498

[13]A. Atrens, M. Liu, N.I.Z. Abidin. Corrosion mechanism applicable to biodegradable magnesium implants. *Mater. Sci. Eng. B,* 176 (2011), pp. 1609–1636

[14]F. Witte, N. Hort, C. Vogt, S. Cohen, K.U. Kainer, R. Willumeit, F. Feyerabend. Degradable biomaterials based on magnesium corrosion. *Curr. Opinion Solid State Mater. Sci.,* 12 (2008), pp. 63–72

[15]M. Yazdimamaghani, M. Razavi, D. Vashaee, L. Tayebi. Development and degradation behavior of magnesium scaffolds coated with polycaprolactone for bone tissue engineering. *Mater. Lett.,* 132 (2014), pp. 106–110

[16]J. Disegi, L. Eschbach. Stainless steel in bone surgery. *Injury,* 31 (2000), pp. D2–D6

[17]K. Yang, Y. Ren. Nickel-free austenitic stainless steels for medical applications. *Sci. Technol. Adv. Mater.,* 11 (2010), p. 014105

[18]M. Sumita, T. Hanawa, S. Teoh. Development of nitrogen-containing nickel-free austenitic stainless steels for metallic biomaterials—review. *Mater. Sci. Eng. C,* 24 (2004), pp. 753–760

Materials Science and Engineering: C, Vol 62 (May 1, 2016): pg. 439-443. DOI.

[19]K. Alvarez, S.-K. Hyun, H. Tsuchiya, S. Fujimoto, H. Nakajima. Corrosion behaviour of lotus-type porous high nitrogen nickel-free stainless steels. *Corros. Sci.,* 50 (2008), pp. 183–193

[20]E. Salahinejad, R. Amini, M. Marasi, M. Hadianfard. Microstructure and wear behavior of a porous nanocrystalline nickel-free austenitic stainless steel developed by powder metallurgy. *Mater. Des.,* 31 (2010), pp. 2259–2263

[21]E. Salahinejad, M. Hadianfard, M. Ghaffari, S.B. Mashhadi, A. Okyay. Liquid-phase sintering of medical-grade P558 stainless steel using a new biocompatible eutectic additive. *Mater. Lett.,* 74 (2012), pp. 209–212

[22]E. Salahinejad, M. Hadianfard, M. Ghaffari, R. Amini, S.B. Mashhadi, A. Okyay. Microstructural characterization of medical-grade stainless steel powders prepared by mechanical alloying and subsequent annealing. *Adv. Powder Technol.,* 24 (2013), pp. 605–608

[23]M. Javanbakht, M. Hadianfard, E. Salahinejad. Microstructure and mechanical properties of a new group of nanocrystalline medical-grade stainless steels prepared by powder metallurgy. *J. Alloys Compd.,* 624 (2015), pp. 17–21

[24]T. Kokubo, H. Takadama. How useful is SBF in predicting in vivo bone bioactivity? *Biomaterials,* 27 (2006), pp. 2907–2915

[25]E. Salahinejad, M.J. Hadianfard, M. Ghaffari, S.B. Mashhadi, A.K. Okyay. Fabrication of nanostructured medical-grade stainless steel by mechanical alloying and subsequent liquid-phase sintering. *Metall. Mater. Trans. A,* 43 (2012), pp. 2994–2998

[26]D.A. Jones. *Principles and prevention of corrosion.* Macmillan (1992)

[27]C. Suryanarayana. Mechanical alloying and milling. *Prog. Mater. Sci.,* 46 (2001), pp. 1–184

[28]R. Amini, E. Salahinejad, M. Hadianfard, M. Marasi, T. Sritharan. Characterization of Fe–Cr–Mn–N amorphous powders with a wide supercooled liquid region developed by mechanical alloying. *Mater. Sci. Eng. A,* 527 (2010), pp. 1135–1142

[29]E. Salahinejad, R. Amini, M. Hadianfard. Structural evolution during mechanical alloying of stainless steels under nitrogen. *Powder Technol.,* 215 (2012), pp. 247–253

[30]R. Amini, E. Salahinejad, E.A. Bajestani, M. Hadianfard. On the general outline of physical properties of amorphous-nanocrystalline Fe–Cr–Mn–N alloy powders prepared by mechanical alloying under nitrogen. *J. Alloys Compd.,* 509 (2011), pp. 3252–3256

[31]E. Salahinejad, R. Amini, M. Marasi, T. Sritharan, M. Hadianfard. The effect of nitrogen on the glass-forming ability and micro-hardness of Fe–Cr–Mn–N amorphous alloys prepared by mechanical alloying. *Mater. Chem. Phys.,* 118 (2009), pp. 71–75

[32]E. Salahinejad, R. Amini, E.A. Bajestani, M. Hadianfard. Microstructural and hardness evolution of mechanically alloyed Fe–Cr–Mn–N powders. *J. Alloys Compd.,* 497 (2010), pp. 369–372

[33]L. Liu, Y. Li, F. Wang. Electrochemical corrosion behavior of nanocrystalline materials—a review. *J. Mater. Sci. Technol.,* 26 (2010), pp. 1–14